Journal of African Earth Sciences 186 (2022) 104421

Contents lists available at ScienceDirect

Journal of African Earth Sciences

journal homepage: www.elsevier.com/locate/jafrearsci

The origin of manganese formations at Çağalali Hill and Kevrïkevr Hill related to the late Triassic rifting of the South Neotethys, SE Turkey: The geological, mineralogical and geochemical components

Burcu Karataş [a,*], Mustafa Akyildiz [a], Nail Yildirim [b], Esra Yildirim [c]

[a] Department of Geology Engineering, Faculty of Engineering, Çukurova University, Adana, 01330, Turkey
[b] General Directorate of Mineral Research and Exploration of Turkey, Department of Mineral Research and Exploration, Ankara, 06520, Turkey
[c] Department of Geology Engineering, Faculty of Engineering, Fırat University, Elazığ, 23119, Turkey

ARTICLE INFO

Keywords:
Southern Neotethys
Manganese mineralization
Geochemistry
Hydrothermal

ABSTRACT

The Koçali Complex includes continental rifting and subduction-related units that make up the southern Neotethys. This complex is a folded, tectonic-segmented succession with lavas, volcaniclastic sediments, pelagic carbonates, radiolarites and manganese deposits (the Tarasa and Konak formations) and ophiolitic units (the Kale formation). Manganese mineralizations in the host formation are found in banded, lenticular and massive forms within red to brown radiolarian cherts. Pyrolusite and polianite are the main manganese minerals, while psilomelane, manganite and minor hausmannite are other manganese minerals. Gangue minerals include quartz and carbonate, with minor barite being observed. The geochemical proofs (MnO: 8.98–73.64%, SiO_2: 3.26–86%) originating from the main oxides indicates a hydrothermal rooted source for the manganese mineralization. This is confirmed by anomalies and trace element patterns including very low Fe/Mn (<0.1), low Co/Zn ratios (mean 0.86), very low ∑REE contents (mean 34.67), slightly negative Eu* value (mean 0.74) and low Ce* value (mean −0.23). Manganese-oxide mineralizations observed in the volcanic sedimentary succession of the Koçali Complex have been interpreted as hydrothermal deposits associated with volcanism during the post-rifting seafloor extension of the southern Neotethys during the Late Triassic period.

1. Introduction

Manganese deposits occur in a range of tectonic environments and are associated with ophiolites (epiophiolitic sequences) as well as continental sedimentary successions. According to the mineralogy, geochemical composition and tectonic environments of these deposits, they are classified as (1) hydrogenous (2) hydrothermal and (3) diagenetic deposits (Polgári et al., 2012; Öksüz, 2011, 2018; Hein et al., 1997; Bolton et al., 1988). Hydrogenous deposits contain ferromanganese crusts depleted in Mn minerals and rich in amorphous iron compounds (Öksüz, 2011; Jach and Dudek, 2005; Usui and Someya, 1997; Toth, 1980). These deposits are characterized by a low Mn/Fe ratio (≦ 1) and high Ni, Cu and trace element concentrations (Hein et al., 1996, 1997; Usui and Someya, 1997; Usui and Nishimura, 1992; Ingram et al., 1990; Toth, 1980). In contrast, hydrothermal deposits precipitate directly from low-temperature hydrothermal solutions and often occur as strata-bound, laminated, irregular bodies and epithermal veins (Hein et al., 1997; Ingram et al., 1990). In modern and ancient marine environments, they are found in spreading centers or in subplate seamounts or island-arc environments associated with subduction (Roy 1992, 1997). Diagenetic deposits exist mainly as nodules, precipitated from hydrothermal solutions or pore waters. These deposits are mostly associated with the oxidation of organic matter and the formation of manganese-carbonate mineralization (Polgári et al., 2012; Öksüz, 2011; Marta Polgári, 1991). Hydrothermal and diagenetic deposits have higher Mn/Fe ratios and a lower trace metal content than hydrogenous deposits (Hein et al., 1994, 1996).

Manganese deposits in Turkey have been described in different geological environments related to the evolution of the Tethys ocean (Öygür, 1990; Öztürk, 1993a,b; Şaşmaz et al., 2014; Öksüz, 2011; Şaşmaz et al., 2014). These beds are (1) hydrothermal and hydrogenetic manganese deposits, hydrothermal and hydrogenetic manganese deposits associated with radiolarian cherts (the İzmir Ankara Erzincan Sutur Belt and Southeast Anatolian orogenic belt) (2) diagenetic manganese deposits

* Corresponding author.
E-mail address: bgoren@cu.edu.tr (B. Karataş).

https://doi.org/10.1016/j.jafrearsci.2021.104421
Received 25 June 2021; Received in revised form 2 November 2021; Accepted 15 November 2021
Available online 20 November 2021
1464-343X/© 2021 Elsevier Ltd. All rights reserved.

associated with black shales in carbonates (Denizli–Ulubat), (3) the hydrothermal manganese deposits in the volcanic sediments of the Black Sea continental-arc and (4) diagenetic manganese deposits found in the Thrace basin–Oligocene deposits (Öztürk 1993a, 2019).

A large number of small to medium sized manganese mineralizations have been reported in the Southeastern Anatolian Orogenic Belt, which also covers the study area (Şaşmaz et al., 2014; Öztürk, 1993a,b Altunbey and Sağıroğlu, 1995; Türkyılmaz, 2004). These are hydrothermal ferro-manganese mineralizations within the Middle Eocene Mineral Complex (Şaşmaz et al., 2014), and the hydrothermal manganese mineralizations within the Upper Triassic–Upper Cretaceous Koçali Complex (Öztürk, 1993a, b; Gören, 2011) (Fig. 1). These manganese deposits from different ages and lithologies are curiously associated with massive seafloor sulfide deposits (e.g. the Maden–Main bed and Adıyaman–Koçali VMS deposits (Fig. 1b). Manganese mineralizations in the Koçali Complex have been known about for 30 years and have been the subject of various studies (Öztürk, 1993a, b; Türkyılmaz, 2004; Yıldırım, 2013a; Gören, 2011; Gören et al., 2010). Manganese mineralizations are within the Upper Triassic–Upper Cretaceous Konak formation, which is the volcanic sedimentary unit of the Koçali



Fig. 1. (a) Ophiolites located in the Alpine–Himalayan orogenic belt (modified according to Dilek and Flower, 2003), (b) Regional geological map showing the SE Anatolian Orogenic Belt (modified according to Yazgan and Chessex, 1991; MTA, 2002) and VMS deposits and manganese/ferro-mangenese mineralizations within the Koçali and Maden complexes (Yıldırım et al., 2016; Türkyılmaz, 2004).

Complex. Their continuity is limited, and they are economically insignificant except for a few deposits with high reserves. On a regional scale, over 50 manganese mineralizations defined in the Konak formation around Adıyaman, Kahramanmaraş, Gaziantep and Kilis are known (Şaşmaz et al., 2014; Yıldırım, 2013a, Fig. 1b).

This study covers the manganese mineralizations of the Koçali Complex, which includes the continental rifting and subduction lithological units of the Late Triassic Age, which form the southern Neotethys. A model is proposed with new field observations together with petrographic descriptions, mineralogy and geochemical (major, trace and REE) data for the Çağalalı Hill and Kevrikevr Hill manganese mineralizations associated with radiolarian cherts.

2. Geological setting

2.1. Regional geological setting and the Koçali Complex

The Anatolian peninsula, which has an important place in the Alpine–Himalayan orogenic system, contains the remains of the Tethys (Paleotethys and Neotethys) oceanic basins, between approximately east to west trending tectonic belts (Pontids, Anatolides, Taurides and Border Folds). The Tethys areas are an oceanic basin that narrows towards the west with the merging of Laurasia in the north and Gondwana in the south in the Permian period (Fig. 1a). Neotethys-related geological events, which formed and closed during the Alpine–Himalayan

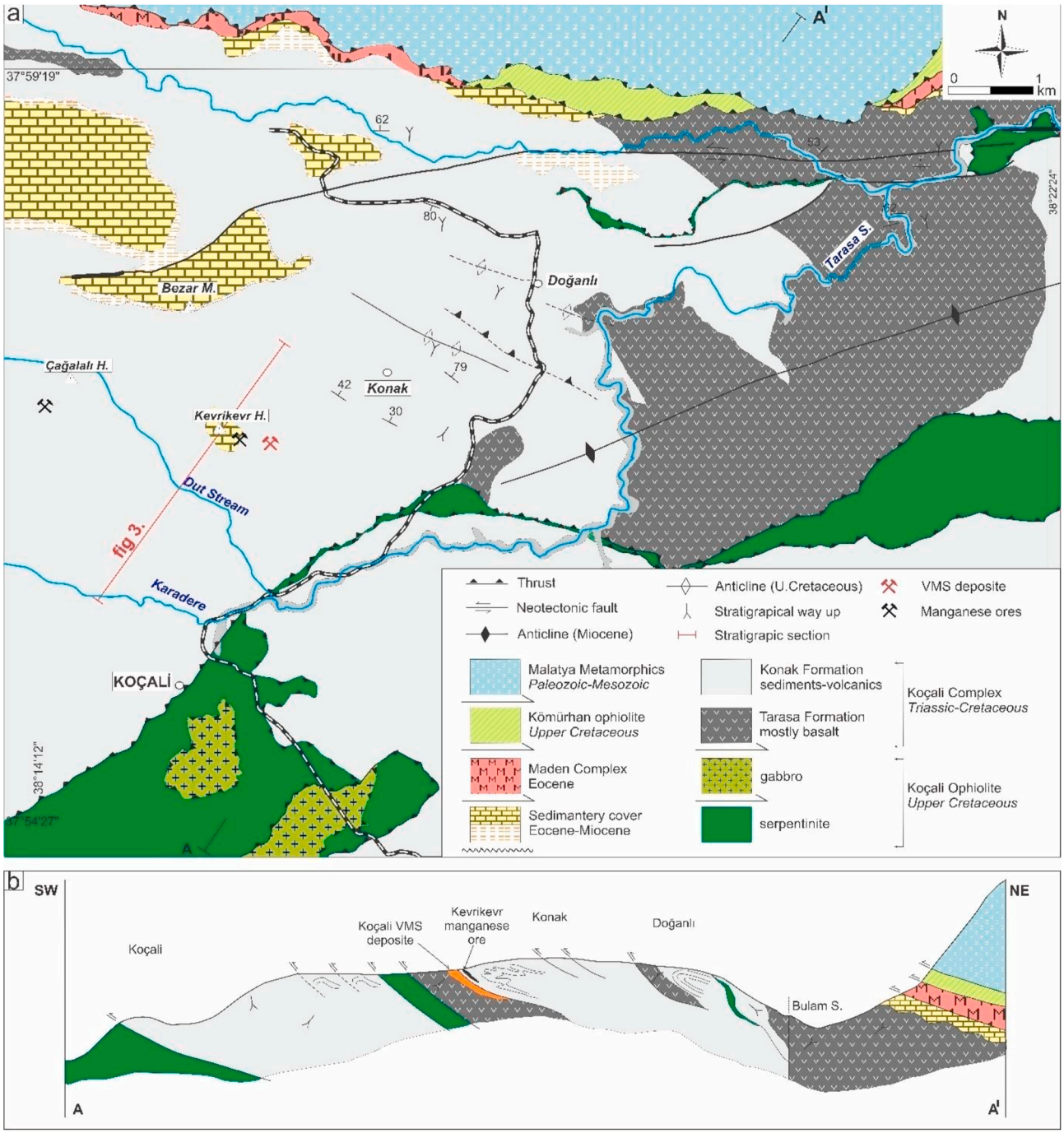


Fig. 2. (a) Summary geological map of the type area of the Koçali Complex, north and northeast of Koçali village, the associated manganese mineralizations and VMS deposits (b) NE–SW directional cross-section summary (Map and cross-section, Robertson et al., 2016b; Yıldırım, 2017 and its references).

orogeny, affected all of Anatolia from the Triassic to the Miocene periods (Şengör and Yılmaz, 1981; Okay and Tüysüz, 1999; Bozkurt, 2001; Robertson et al., 2004; Okay, 2008).

The study area was located within the SEAOB (Southeastern Anatolian Orogenic Belt) in the eastern Mediterranean, which is a part of the Alpine–orogenic system. The SEAOB consists of three different tectonic units, which are approximately east/west trending and separated from each other by the main thrust planes dipping to the north (Yılmaz, 1990, 1993; Yılmaz et al., 1993). In Fig. 1b, these tectonic units are in the nappe zone from north to south, the Condensation Prism, and the Arabian Platform. The area where manganese mineralizations are found is located on the border of the accumulation zone and the Arabian platform, and is represented by different rock groups. In this area, there are different metamorphic units, volcanic sedimentary and ophiolitic units, which may or may not be correlated with each other in terms of lithology, metamorphism, age and location (Fig. 1b). These mainly include – from bottom to top: the Arabian front, the Black Mulberry Complex, the Koçali volcanic sedimentary series, the Koçali ophiolite and the Upper Cretaceous–Middle Miocene aged sedimentary sequence. The metamorphic massifs belonging to the accretion and nappe zone are ophiolites and volcanic sedimentary units (Fig. 1b).

Most of the Late Cretaceous–Cenozoic sedimentary succession transgressively overlies the allochthonous rocks (Black Mulberry and Koçali Complexes) emplaced to the north of the Arabian platform. This transgressive sequence continues in the south over the Arabian front. The deposition on the Arabian platform ended with the southward emplacement of Taurus allochthonous units during the Middle Miocene period. Later, the Late Miocene-, Pliocene- and Pleistocene-aged terrestrial deposits covered the deformed Arabian platform edge and settled allochthonous units (Yıldırım, 2017).

The Koçali Complex, which hosts manganese mineralizations, includes two basic units of different origins, a volcanic sedimentary community (the Tarasa–Konak formations) and an ophiolitic community (the Kale formation). It was formed on the margin of a divergent rift within the outer part of the continental ocean transition zone of the Ladinian–Norian volcanic succession (Tarasa). The Norian–Bajocian volcanic sedimentary succession (Konak) developed in a small Red Sea-type ocean basin during and just after continental rifting (Yıldırım, 2017; Robertson et al., 2016a).

The Koçali ophiolite (Kale) developed in an intra-oceanic subduction

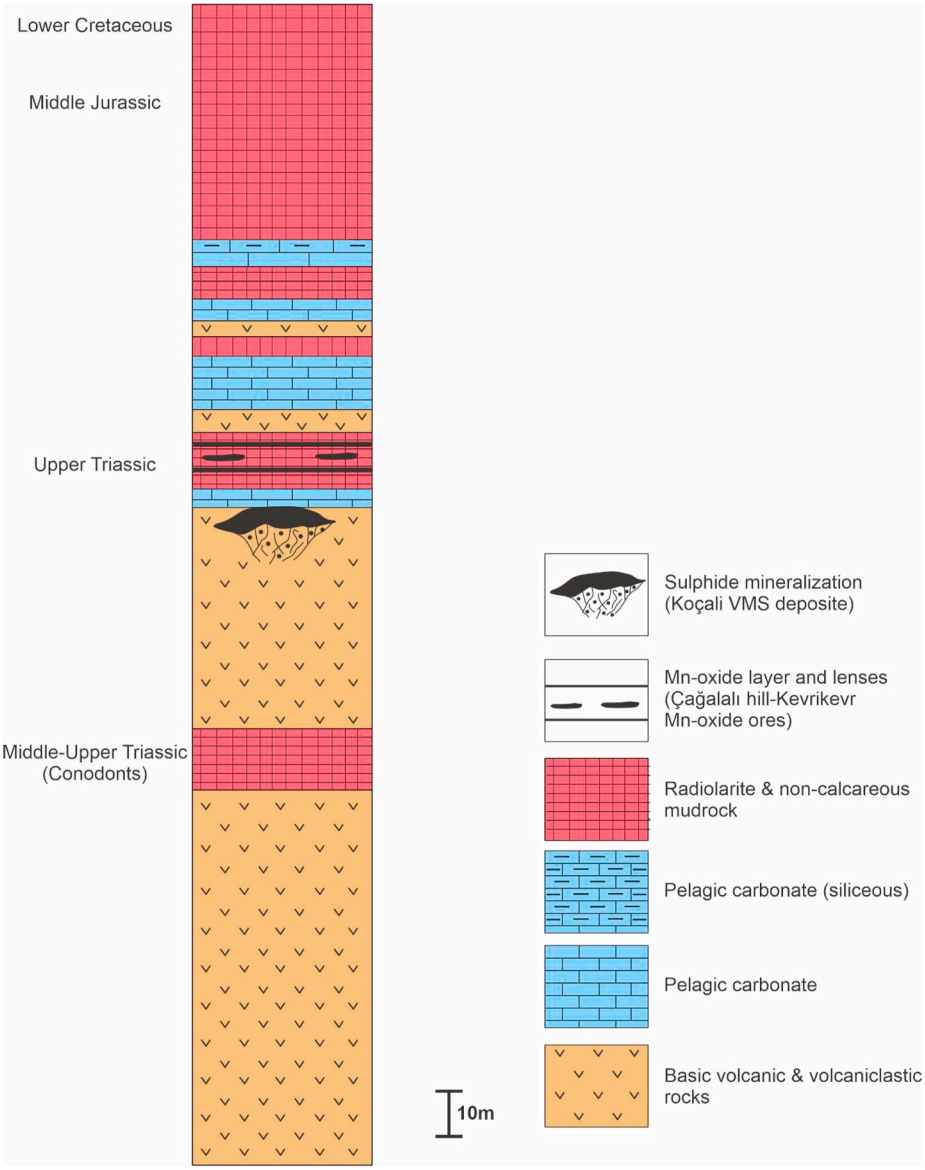


Fig. 3. Simplified log of well-exposed series, associated manganese-oxide and sulfur mineralizations within the type area (Kara dere–Dut dere–Konak village) of the Koçali Complex (see Fig. 2a for log location, modified from Robertson et al., 2016b).

zone between the Arabian platform in the south and the Bitlis–Pütürge microplate in the north, with the northward subduction of the southern branch of the Neotethys during the Late Cretaceous period (Yıldırım, 2017). It is part of the peri-Arabian ophiolite belt, which includes the Bear–Bassit, Kızıldağ and Semail ophiolites.

2.2. Local geological setting

While the basement of the study area and its surroundings forms the Koçali Complex, it is discordantly overlain by Arabian platform deposits (Germav, Gercüş and Hoya formations). The Koçali Complex includes a volcanic sedimentary sequence and ophiolitic rocks that are structurally linked to these units (Fig. 2). The contact between the Tarasa–Konak formations is transitional (Perinçek, 1978; Fourcade et al., 1991; Uzunçimen et al., 2011; Robertson et al., 2016a, b; Yıldırım, 2017) mostly deformed by reverse faults or folding. The Tarasa and Konak formations are widely sheared. The Tarasa formation consists mainly of alternated massive and pillow flow basaltic lava flows. The lavas are interbedded with pelagic limestone, siliceous limestone, radiolarian mudstone (shale) and radiolarite. Overlying the Tarasa formation, the Konak formation consists mainly of basalt, volcaniclastic, dolomitic limestone, radiolarian shale (mudstone), radiolarite and manganese-oxide lenses and layers (Yıldırım, 2017; Robertson, 2016a, Fig. 3). The ophiolitic rocks that emerge as thrust slices in the near south of the study area present an irregular ophiolitic sequence and are represented by serpentinized mantle peridotites and cumulate gabbros (Fig. 2).

2.3. The geology of the Çağalalı Hill and Kevrikevr Hill manganese ores

The Çağalalı Hill and Kevrikevr Hill manganese mineralizations are located approximately 35 km north of Adıyaman province (Fig. 1b) and were exploited for a period. However, the actual size of these beds is unknown. The manganese mineralizations extend approximately east to west and are located approximately 2 km apart (Fig. 2a). The Konak formation hosts beds and thick basaltic volcanic–volcaniclastic rocks that are located at the base of the succession. It consists of gray-pink pelagic limestone, siliceous limestone, dolomitic limestone, radiolarian shale, strip radiolarites and manganese-oxide layers in these radiolarites towards the top. Basalts are interbedded with pelagic limestone, siliceous limestone and radiolarites. The ages of the radiolarian sediments and conodonts are from the Middle–Upper Triassic to the Lower–Middle Jurassic and Upper Cretaceous periods (Fourcade et al., 1991; Uzunçimen et al., 2011 Robertson et al., 2016b, Yıldırım, 2017, Fig. 3).

Manganese-oxides in radiolarites are found in layered, banded, lenticular and massive forms. The Çağalalı Hill manganese mineralizations are also in the form of irregular lenses and alternating layers within the radiolarites (Fig. 4b). These mineralizations are approximately from the east to a 45° north/west position and were fractured, folded (Fig. 4c) and fragmented together with the host rock. This indicated an important tectonism and deformation after the formation of mineralizations. The ore is brittle, metallic lustrous, lead-gray and slightly reddish.

The manganese mineralizations of Kevrikevr Hill are similar to those of Çağalalı Hill and are located at 70° north to the east–west line. It is

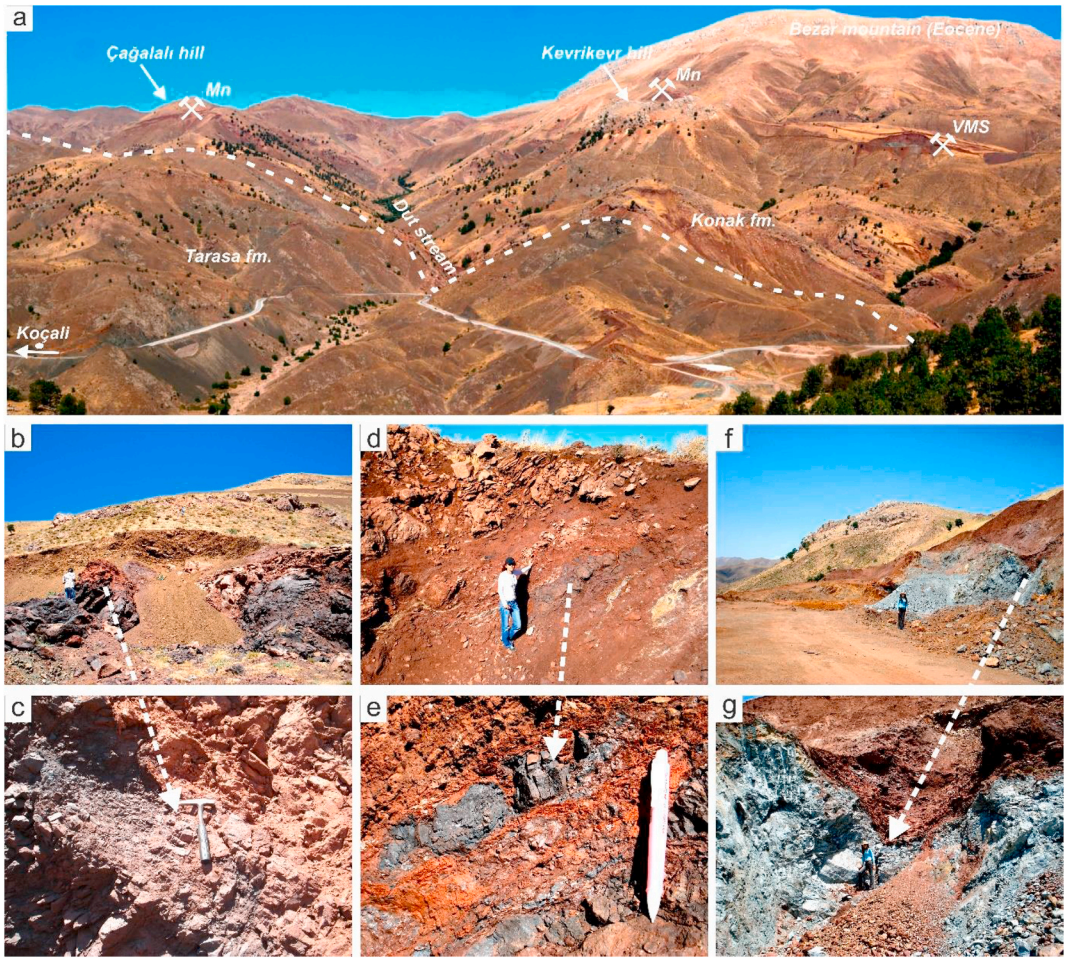


Fig. 4. (a) Field view showing the type area and associated mineralizations of the Koçali Complex (looking west upstream from the Mulberry Stream) (b) manganese mineralization observed as irregular lenses in the radiolarians at Çağalalı Hill, and (c) the wall–rock relationship (d) the layered/banded manganese mineralization with thicknesses ranging from 5 cm to 30–40 cm at Kevrikevr Hill and (e) coiled and fragmented manganese ore compatible with the host rock, (f, g) massive ore and ceiling rock (radiolarian/non-calcareous mudstone).

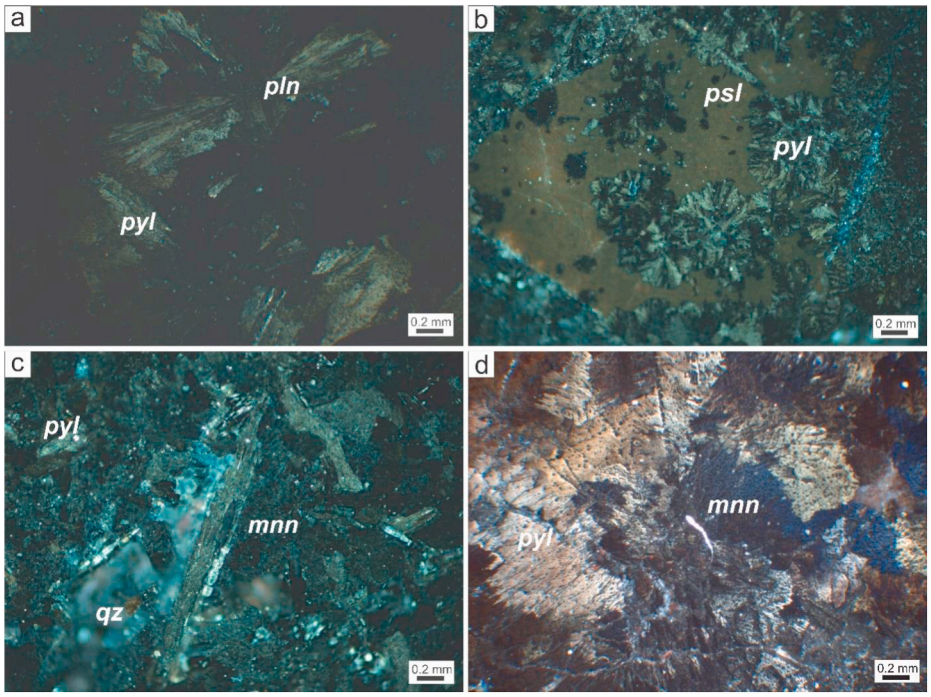


Fig. 5. (a) Medium-coarse crystalline, rod, radial–radial shaped pyrolocyte and twin lamellar, short-prismatic grained, bundle-shaped radial-looking polianite (viewed under cross-polarized light) (b) well-developed crystalline psilomelane (viewed under cross-polarized light) intertwined with pyrolusite (c, d) manganite intertwined with pyrolusite – sometimes transformed into pyrolusite (mineral abbreviations: pyl = pyrolusite, pln = polianite, psl = psilomelane, mnn = manganite, qz = quartz).

layered and/or banded, with thicknesses ranging from 5 cm to 30–40 cm and in lengths from 1.5 to 2 m (Fig. 4d). The ore is compatible with the bedrock and is folded and fragmented (Fig. 4e). Manganese hand samples show metallic luster and were black and blackish-brown in color.

In addition, sulfide mineralization (Cu, Zn) is located between the basalts (basement rock) belonging to the volcanic sedimentary series and the overlying deep-sea pelagic sediments (ceiling rock) in the near east (~500 m) of Kevrikevr Hill (Figs. 3 and 4a to g). The mineralizations presented a distinctive facies with gossan (proximal) seafloor oxidation products and sulfide breccia (proximal), massive ore (proximal), vents (proximal), sulfide sandstone (distal) and stockwork ore structure (Yıldırım, 2013b, 2017; Yıldırım et al., 2016). These mineralizations have been reported to be similar to sea-floor volcanogenic massive sulfide (VMS) deposits, which are products of rifting and which spread slowly in mid-ocean ridge environments (İlhan, 2013; İlhan et al., 2016; Yıldırım, 2013b, 2017; Yıldırım et al., 2016).

3. Sampling and analytical methods

During the field studies, 12 ore and 6 side-rock samples were taken for mineralogical-petrographic and geochemical studies. Samples for geochemical analyzes were prepared in the geochemistry laboratory of the Department of Geological Engineering, part of the Faculty of Engineering and Architecture in Çukurova University. Major, trace and rare earth element contents of a total of 18 samples were analyzed in the Acme Analytical Laboratories (CANADA). These included 8 ore and 3 host rock samples from Çağalalı Hill, and 4 ore and 3 host rock samples from Kevrikevr Hill. The major elements were measured using an X-Ray fluorescence (XRF) technique on pellets obtained by adding 1/5 sample and Lithium tetraborate (Li2B4O7) to a platinum–gold crucible at 1500 °C. Trace elements on pressed pellets were analyzed by the same method. Rare earth elements were measured by the ICP-MS method.

Thin sections were prepared in order to determine the mineralogical composition and textural properties of the wall-rock samples (5 pieces) taken for mineralogical and petrographic examinations. In order to determine mineral paragenesis and succession, 9 bright sections were prepared from the ore samples. The preparation and examination of thin and bright sections were carried out in the Department of Geological Engineering laboratories of Çukurova University.

4. Discussion

4.1. The mineralogy of manganese ores

The predominant manganese-oxide minerals are pyrolusite and polianite, with lesser psilomelane, manganite and minor hausmannite. Gangue minerals included common quartz and carbonate, and minor barite. Pyrolusite is the most predominant ore mineral and is in the form of medium to coarse crystals. The rods are radial–radial in shape (Fig. 5a–d) and sometimes cut by quartz veins (Fig. 5c). It has very strong anisotropy and is yellowish, dark brown and greenish-blue. At least some of the pyrolusite developed primarily from the oxidized solutions developed secondary to manganite. Polianite is the most common manganese mineral after pyrolusite. It is distinguished from its similarity to pyrolusite by showing twin lamellae. They are mostly short prismatic grains with a bunch-shaped radial appearance (Fig. 5a). They show pleochroism in yellowish-, bluish-, brownish- and greenish-gray colors. Its anisotropy is gray, orange and bluish. Psilomelane usually shows intergrowths with pyrolusite (Fig. 5b). It is in the form of well-developed crystals and mostly in the form of radial rods. Generally, pyrolusite–psilomelane–manganite association is common. It has strong anisotropy and is whitish-gray in color. Manganite is usually brownish-

Table 1
Major oxide contents of ore samples. Fe/Mn ratio (%) and Trace element contents of ore samples (ppm) (Ç: Çağalalı Hill, B: Kevrikevr Hill).

Sample	SiO_2	Al_2O_3	Fe_2O_3	MgO	CaO	Na_2O	K_2O	TiO_2	P_2O_5	MnO	Cr_2O_3	LOI	Mn	Fe	Fe/Mn	Mn/Fe	Ba	Co	Sr	Th	U	Zr	Cu	Pb	Zn	Ni	Co/Zn	Co/Ni
Ç1	59.7	0.38	0.1	0.53	16.18	0.02	0.04	0.01	0.03	8.98	0.002	13.8	6.95	0.07	0.01	99.29	1.4	58	64	0.2	0.3	15	46	4.8	38	42	1.53	1.38
Ç5	80.9	0.21	0.12	0.05	3.99	0.02	0.03	<0.01	0.02	19.26	<0.002	5.3	14.91	0.08	0.01	186.38	810	5.1	19	0.2	0.7	9.3	36	0.6	62	37	0.08	0.14
Ç6	5.67	0.74	<0.04	0.54	0.69	<0.01	0.05	<0.01	0.03	69.67	<0.002	12.7	53.95	0.07	0.001	770.71	5.7	99	85	0.4	2.4	34	242	0.9	302	290	0.33	0.34
Ç9	3.47	0.5	<0.04	0.2	0.52	<0.01	0.01	<0.01	0.06	73.64	<0.002	12.9	57.02	0.08	0.001	712.75	4.7	41	80	0.3	1.5	61	94	0.5	307	206	0.13	0.2
Ç10	3.26	0.39	<0.04	0.16	1.25	0.01	0.02	<0.01	0.05	71.54	<0.002	13.2	55.39	0.07	0.002	791.29	9	49	111	0.3	1.1	16	73	0.5	298	267	0.17	0.18
Ç14	86	0.75	0.6	0.74	0.44	0.07	0.12	0.04	0.06	17.87	<0.002	3.3	6.09	0.08	0.01	76.13	197	80	70	1.7	2.4	93	21	4.5	54	60	1.48	1.01
Ç15	19.6	0.34	<0.04	0.16	0.63	0.01	0.02	0.02	0.01	67.77	0.003	11.3	52.47	0.06	0.001	874.5	38	41	152	0.5	4.7	185	327	2	257	90	0.16	0.45
Ç16	77.1	0.1	<0.04	0.03	0.31	0.02	<0.01	<0.01	0.03	19.92	<0.002	2.4	15.42	0.08	0.005	192.75	433	59	41	0.2	6.8	18	72	8.8	29	31	2.04	1.91
B1	46.3	0.56	23.26	0.72	11.94	0.02	0.05	0.02	0.09	14.65	<0.002	12.2	11.34	0.07	0.01	162	539	125	59	0.3	0.6	94	86	8.9	150	153	0.83	0.82
B3	41.5	0.61	0.19	1	21.02	0.02	0.04	0.03	0.03	15.73	<0.002	17.8	12.18	0.08	0.01	152.25	18	119	349	0.4	0.3	18	80	4.7	64	82	1.86	1.45
B5	71.5	0.22	4.71	0.32	5.42	<0.01	0.03	<0.01	0.05	11.25	<0.002	6.2	8.71	0.07	0.01	124.43	2.4	96	30	0.2	0.8	43	159	7.4	69	123	1.39	0.78
B11	77.1	0.8	0.38	0.46	0.22	0.04	0.08	0.03	0.03	16.87	<0.002	3.8	13.06	0.07	0.01	186.57	1.3	36	90	0.6	3.1	104	64	6.1	110	31	0.33	1.16

gray in color and is rod-shaped. They also show intertwined, co-developed and sometimes pyrolusite transformations with pyrolusite (Fig. 5c.d). Hausmannite is the rarest Mn-oxide mineral. It shows a greenish-gray anisotropy.

Gangue minerals are predominantly quartz and minor barite with lesser amounts of carbonate. Quartz is usually crushed due to deformation and is seen in crypto-crystalline to micro-crystalline forms. Quartz crystals are present as void fillers or in the interstitial spaces of manganese minerals (Fig. 5c). Carbonate is mostly composed of calcite in irregular forms filling the veins and cracks in the Mn-oxide matrix. Barite is very rare and occurs as a void filler in manganese-rich zones.

Çağalalı Hill and Kevrikevr Hill manganese-oxide mineral associations are composed of pyrolusite, polianite, psilomelane, manganite and hausmannite and are similar to the mineral association developed due to hydrothermal systems.

4.2. Major and trace elements in the manganese oxides

The main oxide and trace element contents of Mn-oxide ore samples associated with the Koçali Complex are given in Table 1. Accordingly, the MnO ratio varies from 8.98% to 73.64%; an average of 33.92%. The SiO_2 ratio of the same ores is in a range from 3.26% to 86% with an average of 47.62%. The fact that the host rocks are radiolarite and radiolarian cherts increases the SiO_2 content of the samples. The Fe/Mn ratio is used to determine the formation environments of manganese deposits. In studies on manganese mineralizations with different formations, the Fe/Mn ratio of mineralizations was determined to be around 1 in hydrogenetic deposits precipitated slowly from sea water, and <0.1 in submarine hydrothermal deposits. Fe/Mn < 0.1 is explained by the rapid precipitation of hydrothermal solutions in submarine hydrothermal centers. Fe/Mn ratios of manganese ore samples from Kevrikevr Hill and Çağalalı Hill located in the Koçali Complex were <0.1 (Table 1). The small scale of this value caused the separation of Fe and Mn since Fe is less soluble than Mn in sea water, and the dominance of Mn over Fe in manganese oxide ores, and the very low Fe/Mn ratios, indicated that they were formed by rapid precipitation from hydrothermal solutions in submarine hydrothermal centers, which in turn generally indicates that there were submarine hydrothermal formations.

When the trace element contents of the manganese mineralizations of Kevrikevr Hill and Çağalalı Hill associated with the Koçali Complex were examined. The contents were as follows: Ba from 5.79 to 17.586 ppm, with an average of 3.190 ppm; As from 0.8 to 89.6 ppm, with an average of 15.07 ppm; Sr from 19.2 to 348.8 ppm, with an average of 92.62 ppm; Zn from 29 to 307 ppm, with an average of 145 ppm; Pb from 0.5 to 8.9 ppm, with an average of 4.14 ppm; Ni from 31 to 290 ppm, with an average of 117.6 ppm and Co from 5.1 to 124.90 ppm, with an average of 59.8 ppm.

In order to distinguish the formation types of the manganese deposits (hydrogenetic or hydrothermal) from each other, separation diagrams were used by making use of some main element and trace element contents (Fig. 6). Mn-oxide deposits (hydrothermal and hydrogenetic) are easily separated depending on the ratio of trace elements – such as Co, Zn and Ni – to each other (Choi and Hariya, 1992). High Ni and Zn values indicate hydrothermal deposits, while relatively high Co values are indicative of hydrogenetic deposits (Fig. 6 a). Sedimentary exhalative deposits and manganese nodules were distinguished in the Fe–Mn-(Ni + Co + Cu)*10 diagram. Condensation of elements such as Ni, Co, Cu is much lower in hydrothermal beds than in hydrogenetic beds (Bonatti et al., 1976). Due to these low values, the ore samples fall into the hydrothermal area (Fig. 6 b). Al in the environment is formed from clay minerals in sedimentation, and therefore very low Al values in a deposit indicate that mineralization can only be formed by hydrothermal activity (Bamba, 1984). Accordingly, all of the ore samples fall into the hydrothermal area due to their low Al and high Si contents (Fig. 6 c). In the Co/Zn – Co + Ni + Cu diagram used to separate the hydrothermal and hydrogenetic deposits, the samples are also

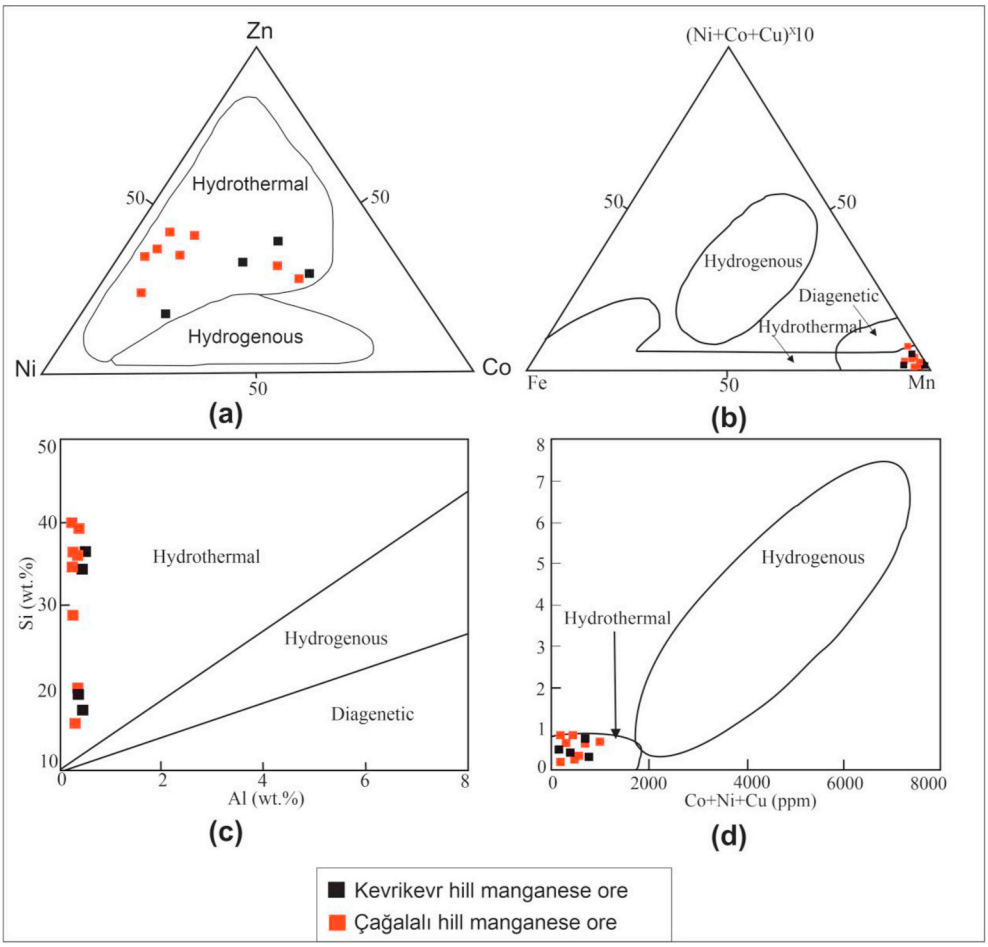


Fig. 6. The ternary discrimination diagrams prepared using the major and trace element concentrations (a) Zn–Ni–Co discrimination diagram (Choi and Hariya, 1992) (b) Fe–Mn–(Ni + Co + Cu)*10 discrimination diagram (Bonatti et al., 1976) (c) Si–Al discrimination diagram (Peters, 1988) and (d) Co/Zn–Co + Ni + Cu discrimination diagram (Toth, 1980).

concentrated in the hydrothermal field (Toth, 1980), (Fig. 6 d).

The average major and trace element contents of some manganese deposits in the world that have been formed from different origins were compared to the average major and trace element contents of the Çağalalı Hill and Kevrikevr Hill manganese mineralizations. The trace element (Ni, Co, Cu, Zn) contents of hydrothermal deposits are lower than hydrogenetic deposits (Crerar et al., 1982). Accordingly, the SiO_2 content of the sedimentary manganese deposits should be lower than the hydrothermal deposits, and the MnO_2 and Al_2O_3 content should be higher. Major element and trace element concentrations of the mineralizations in the study area were compatible with submarine hydrothermal deposits (Table 2).

4.3. Rare earth elements in the manganese oxides

The Rare Earth Element (∑REE) data for manganese ore and host rocks from Kevrikevr Hill and Çağalalı Hill associated with the Koçali Complex are given in Table 3. The values used in all calculations in distribution profiles use the Evensen et al., (1978) chondrite values and are presented graphically in Fig. 7. The total Rare Earth Element (∑REE) contents of 12 manganese ore samples in the study area ranged from 5.85 to 94.98 ppm, with an average of 34.67. These values are considerably lower than the values in hydrogenetic and early diagenetic deposits. In hydrogenetic and early diagenetic deposits, these values are several thousand ppm.

As can be seen in the chondrite-normalized REE diagram, the manganese ore samples from Kevrikevr Hill and Çağalalı Hill showed a negative Eu (Europium) anomaly. Eu anomalies, Eu *, are calculated with the formula Eu norm./(2/3Sm norm.+1/3Gd norm). Eu * values ranged from 0.29 to 1.71, with an average of 0.74. These values were higher than those in sea water and are similar to hydrothermal solutions. Eu/Eu* values were calculated with the formula Eu norm./(Sm norm.+ Gd norm.)/2 (Mills et al., 2001). These values ranged from 0.26 to 1.60, with an average of 0.76. The Eu/Eu* values in the host rocks ranged from 0.52 to 0.69, with an average of 0.56. These values indicated to us a hydrothermal contribution to the formation of the ores and host rocks. The negative Eu anomaly observed in the ore samples showed that the temperature of the solution in which the ores precipitated did not rise above 250 °C. A positive Eu anomaly represents higher temperatures (Usui and Someya, 1997). Eu is an element found in high concentrations in many hydrothermal formations. The Eu/Sm ratio is used to express the role this element plays as an indicator of the hydrothermal effect (Varentsov, 1993). Eu/Sm values in the ore samples in the study area ranged from 0.14 to 1.23, with an average of 0.43 species (Table 3).

Table 2
Major and trace element contents of various type Mn–Fe deposits.

	Guichi Sedimentar (China) (Jiancheng et al., 2006)	Ulukent Sedimentar (Turkey) (Kuşçu and Gedikoğlu, 1989)	Hazara Hydrothermal-Hydrogenous (Shah and Moon, 2007)	Binkılıç Sedimentar-Diagenetic (Turkey) (Öztürk and Frakes, 1995)	Baby Bare Hydrothermal (Northeast Pasific Ocean) (Fitzerald and Gills, 2006)	Çayırlı Hydrothermal (Turkey) (Öygür, 1990)	Maden Complex Ferromanganese Deposits (Turkey) (Şaşmaz et al., 2014) (The average of Kom deposits in the Maden Complex)	Çağalalı Hill and Kevrikevr Hill manganese deposits (this study)
SiO_2	–	13.68	9.41	10.65	2.02	63.02	22.40	50.6
TiO_2	–	0.1	0.84	0.02	0.04	0.03	0.13	0.02
Al_2O_3	–	2.49	12.53	0.28	0.27	0.65	3.85	0.45
Fe_2O_3	–	3.72	20.33	2.46	2.3	0.68	34.26	0.98
MnO	–	63.78	33.78	33.39	48.52	29.22	20.10	32.08
MgO	–	1.99	0.59	1.27	1.58	0.2	1.26	0.39
CaO	–	4.05	6.43	18.96	0.97	0.24	7.30	4.83
Na_2O	–	0.24	0.07	0.39	0.64	0.05	0.15	0.02
K_2O	–	0.05	0.88	0.56	0.22	0.11	0.07	0.04
P_2O_5	–	0.18	0.73	0.31	0.04	0.04	1.33	0.04
Ba	13.786	427	6304	6892	7091.67	1229.4	672.1	3595
V	258	–	573	106	172.33	143.7	968.1	93.92
Cr	10	–	247	26	8.89	13.7		63.4
Co	2	13	404	56	135.33	25.21	60.6	107.3
Ni	28	10	305	167	300.67	69.4	686.2	102.39
Cu	50	56	375	26	226	154.9	499.2	132.76
Zn	26	70	580	49	123.22	66.7	343.3	3.96
Pb	112	65	23.57	–	–	60.5	159.9	0.41
Th	2	–	31	–	1	0.4	1.7	0.77
Rb	2	–	24	–	14.22	2.9		92.62
Sr	85	185	–	2100	877.44	243.4	907.1	6.63
Y	5	–	–	15	10	33		11.69
Nb	3	–	–	11.1	1.5	0.7		35.27
Zr	12	–	–	32	9.22	4	68.6	15.07

Eu/Sm values are not higher than 0.23 to 0.26 in Mn–Fe nodules of hydrogenetic, hydrogenetic-diagenetic and diagenetic origin. Eu/Sm values in high temperature hydrothermal fluids in the axial zone of the East Pacific Rise range from 2.19 to 3.18. However, when these liquids are mixed with sea water, the Eu/Sm ratio drops to 0.95 (Varentsov, 1993). The Eu/Sm ratio of the ore samples in the study area is high, indicating that the samples are supported by hydrothermal vents.

As can be seen in the chondrite-normalized REE diagrams, the ore samples associated with the Koçali Complex show negative anomalies for Ce (Fig. 7). In the chondrite-normalized REE diagrams, Çağalalı Hill manganese samples are clustered in two different groups. In terms of REE, one group was more enriched than the other group. The reason for this is that the samples in the group that were more enriched in terms of REE were more distal and have more seawater interaction, that is, more seawater input. A positive Ce anomaly is a characteristic feature in hydrogenetic deposits, and a negative Ce anomaly is a characteristic feature in hydrothermal deposits. The Ce* values in manganese ore samples from Kevrikevr Hill and Çağalalı Hill associated with the Koçali Complex were calculated with the formula Ce norm./(2/3La norm.+1/3Pr norm.), Ce* values ranged from 0.23 to 2.11, with an average of 0.71 (Table 3). These low values reflected the accumulation of mineralization under a low redox potential from a well-oxygenated and stagnant water body. A Ce anomaly > -0.1 indicated hydrogenetic deposits, whereas a Ce anomaly< -0.1 indicated hydrothermal deposits (calculated with the Ce anomaly formula: log(3 × Ce norm./(2 × La norm.+Nd norm.)). In the mineralizations in the study area, the Ce anomaly was −0.23 on average.

∑LREE/∑HREE ratios, Ce/La and Y/Ho values are given in Table 3. The ∑LREE/∑HREE ratio indicated initial enrichment during the manganese oxidation processes, and the ∑LREE/∑HREE positive correlation was also responsible for REE uptake during ore formation. LREEs were obtained from volcaniclastics, while HREEs were obtained from MnO_2 formed by precipitation in seawater. The ratio of ∑LREE/∑HREE in the ore samples in the study area ranged from 1.30 to 12.19, with an average of 4.84. LREE > HREE indicated that the mineralization was formed by hydrothermal solutions. The La norm./Nd norm. ratio in the ore samples varied from 2.08 to 4.25, with an average is 2.79. The Dy norm./Yb norm. ratio varied from 0.70 to 1.67, with an average of 1.19. These values are 3.0–7.4 (mean 4.5) and 0.6 to 2.1 (mean 1.2) in hydrothermal solutions, respectively, and when compared, it supports the premise that the source of manganese mineralizations in the study area were hydrothermal. The Ce/La and Y/Ho ratios of mineralization are on average, 1.48 and 20.74, respectively. This indicated that there was more than one source in mineralization or that substances from outside were mixed into the environment, and these rates increased where there was an increase in terrigenous substances. In the mineralizations, these ratios were at normal values and showed that there was no external substance mixture.

4.4. Genetic model of the Koçali Complex manganese mineralizations

Evidence of continental rifting and subduction (SSZ) in the Triassic period, which formed the southern Neotethys, was found within the Koçali Complex. Rifted divergent continental margin volcanics (Tarasa Formation) and deep sea sediments (Konak Formation) developed in a small Red Sea-type ocean basin during and just after continental rifting (Yıldırım, 2017; Robertson et al., 2016a,b). Interbedded fine-grained carbonates came from the Arabian carbonate platform as low-intensity gravity flows, while radiolarian sediments containing manganese mineralizations were deposited below the carbonate equilibrium depth

Table 3
REE analysis results of ore and wall-rock samples.

	La	Ce	Pr	Nd	Sm	Eu	Gd	Tb	Dy	Ho	Er	Tm	Yb	Lu	Y	∑REE	Eu/Sm	Ce*	Eu*	Eu/Eu*	Cean.	∑LREE /∑HREE	LaN/NdN	Ce/La	DyN/YbN	Y/Ho
Ç1	2.2	2.2	0.44	2.2	0.54	0.18	0.94	0.18	1.16	0.23	0.62	0.08	0.45	0.07	6.3	11.49	0.33	0.46	0.8	0.77	−0.34	2.08	2.94	1	1.67	27.39
Ç5	0.6	0.5	0.08	0.4	0.12	0.04	0.2	0.04	0.28	0.07	0.22	0.03	0.24	0.03	1.9	5.85	0.33	0.41	0.82	0.78	−0.38	1.56	2.91	0.83	0.76	27.14
Ç6	1.2	3.2	0.29	1.2	0.54	0.17	0.96	0.22	1.35	0.3	1.01	0.15	0.93	0.15	5.2	11.67	0.31	1.17	0.75	0.71	0.08	1.3	2.94	2.66	0.94	17.33
Ç9	1.2	2.4	0.2	0.7	0.35	0.05	0.88	0.2	1.28	0.3	1.01	0.16	1.18	0.18	5.6	10.09	0.14	0.95	0.29	0.26	0	1.94	3.32	2	0.7	18.66
Ç10	1.8	2.5	0.29	1.3	0.48	0.28	1.49	0.34	2.3	0.55	1.6	0.25	1.57	0.23	8.6	14.98	0.58	0.66	1.07	0.93	−0.17	2.79	2.68	1.38	0.95	15.63
Ç14	8.8	18.9	1.81	7.3	1.4	0.24	1.34	0.24	1.42	0.28	0.84	0.15	0.93	0.13	6	43.78	0.77	0.98	0.5	0.7	−0.68	3.29	1.94	0.45	1.52	35.61
Ç15	13.8	61.8	2.4	8.7	1.82	0.35	2.08	0.36	1.66	0.3	0.74	0.12	0.74	0.11	5.1	94.98	0.19	2.11	0.54	0.71	−0.82	2.84	3.7	0.33	1.5	33.56
Ç16	18.6	9	3.2	13.3	2.87	0.51	3.03	0.58	3.3	0.53	1.57	0.25	1.61	0.23	7.3	58.58	0.17	0.23	0.51	0.73	−0.65	3.45	2.09	0.47	1.64	36.95
B1	7.4	4	1.43	6.3	1.38	0.38	1.85	0.33	1.91	0.41	1.18	0.19	1.2	0.18	11.7	28.14	0.74	0.25	0.73	0.73	−0.59	2.88	2.28	0.54	1.03	28.52
B3	3.8	3.8	0.76	3.1	0.86	0.64	1.68	0.3	1.68	0.4	1.04	0.14	0.76	0.1	9.8	19.06	1.23	0.46	1.71	1.6	−0.32	2.12	2.37	1	1.44	24.5
B5	6.5	7	1.17	5.6	1.04	0.29	1.28	0.22	1.37	0.3	0.86	0.12	0.78	0.11	8	26.64	0.28	0.5	0.76	0.77	−0.29	4.28	4.25	1.07	1.14	26.66
B11	26.6	25.6	5.93	21.7	3.54	0.53	2.45	0.38	1.91	0.31	0.85	0.13	0.74	0.11	5.9	90.78	0.15	0.43	0.47	0.56	−0.48	5.81	2.08	0.71	1.41	12.63
Ç3	29.5	10	7.32	33.7	7.84	2.04	9.77	1.56	8.94	1.74	4.71	0.68	3.87	0.55	58.4	122.2	0.26	0.15	0.7	0.52	−0.34	12.19	2.37	0.96	1.68	19.03
Ç17	11.4	5.2	2.49	11.4	2.4	0.64	3.22	0.48	2.83	0.57	1.5	0.21	1.21	0.17	20.3	43.72	0.26	0.21	0.71	0.53	0.08	7.21	2.34	2.14	0.99	21.42
Ç20	9.7	4.6	2.26	9	2.06	0.55	2.59	0.39	2.29	0.46	1.23	0.16	0.91	0.12	17	36.32	0.27	0.21	0.72	0.55	0.34	14.54	3.07	4.47	1.46	17
B7	14.7	10.5	3.17	13.7	2.67	0.47	2.32	0.4	2.28	0.38	1.04	0.15	1.05	0.15	4.8	52.98	0.17	0.32	0.53	0.53	−0.62	4.27	2.71	0.48	1.33	13.77
B8	2.5	6.9	0.51	1.9	0.54	0.1	0.49	0.09	0.55	0.13	0.34	0.05	0.35	0.06	3	14.51	0.18	1.26	0.55	0.69	−0.69	3.27	1.74	0.45	1.57	34.9
B9	10.5	4.8	2.46	11.7	2.6	0.65	3.15	0.47	2.86	0.55	1.44	0.2	1.18	0.15	19.2	42.71	0.25	0.2	0.68	0.58	0.12	6.04	2.55	2.76	1.02	23.07
MİN.	0.6	0.5	0.08	0.4	0.12	0.04	0.2	0.04	0.28	0.07	0.22	0.03	0.24	0.03	1.9	5.85	0.14	0.23	0.29	0.26	−0.82	1.3	1.94	0.33	0.7	12.63
MAX.	26.6	61.8	5.93	21.7	3.54	0.64	3.03	0.58	3.3	0.55	1.57	0.25	1.61	0.23	11.7	94.98	1.23	2.11	1.71	1.6	0.08	5.81	4.25	2.66	1.67	36.95
AVE.	7.70	11.74	1.5	5.98	1.245	0.3	1.51	0.28	1.63	0.33	0.96	0.14	0.92	0.13	6.78	34.67	0.43	0.71	0.74	0.76	−0.38	2.86	2.79	1.03	1.22	25.37

Eu*:Eu_{norm}/(2/3Sm norm.+1/3Gd norm.).Ce*:Ce_{norm}/(2/3La_{norm}+1/3Pr_{norm}.) ∑REE:La + Ce + Pr + Nd + Sm + Eu + Gd + Tb + Dy + Ho + Er + Tm + Yb + Lu (Normalize values Evensen,1978). ∑LREE/∑HREE: (La + Ce + Pr + Nd + Sm + Eu) + (Gd + Tb + Dy + Ho + Er + Tm + Yb + Lu). Çağalalı Hill ore: Ç1, Ç5, Ç6, Ç9, Ç10, Ç14, Ç15, Ç16. Çağalalı Hill Wall-rocks: Ç3, Ç17, Ç20 Ceanom: log (3xCe_{norm}/(2La_{norm} + Nd_{norm}) Kevrikevr ore: B1, B3, B5, B11. Kevrikevr wall-rocks: B7, B8, B9.

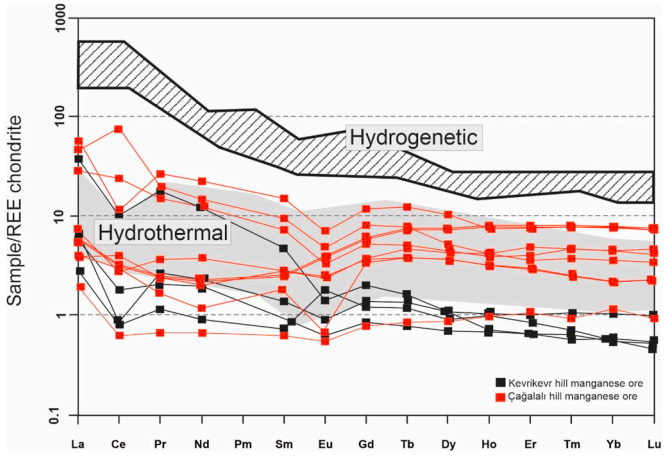


Fig. 7. Spider diagram of Kevrikevr Hill and Çağalalı Hill manganese ore samples (Evensen et al., 1978) and REE diagram showing hydrogenous and hydrothermal fields (Von Stackelberg, 1997).

(Yıldırım, 2017; Robertson et al., 2016a, b). The ophiolitic rocks (Kale Formation) were contemporaneous with the peri-Arabian ophiolites, including Kızıldağ, the Eastern Troodos (Cyprus), Bear Simple (Syria) and Samail (Oman) ophiolites in the Eastern Mediterranean region and developed in the intraoceanic subduction zone in the southern Neotethys (Yıldırım, 2017).

Medium-scale Cyprus-type VMS mineralizations (Adıyaman–Sincik–Ormanbaşı Hill, Adıyaman–Koçali, Diyarbakır–Çüngüş–Derdere and Gaziantep–Ortaklar) defined within the Koçali Complex have been reported (Şaşmaz et al., 1999; Yıldırım, 2013b; Yıldırım et al., 2012, 2016; İlhan, 2013). Similar mineralizations are known along the Tethys suture zone (Yıldırım et al., 2016 and in references). The Adıyaman–Koçali VMS deposit is very close (~500m) to the Çağalalı Hill and Kevrikevr Hill manganese mineralizations and is within the radiolarian cherts, which is the ceiling rock of the massive sulfide mineralizations.

Rock/sea water interaction is important in seabed massive sulfide mineralizations. This interaction produces major mineralogical and geochemical alterations. These circulating fluids mix with high temperature solutions associated with volcanic activity, rise through fractures and fissures under the influence of adiabatic pressure, and then reach the seafloor and spread. The downward circulation of seawater along fractures in the oceanic crust and its interaction with the crust cause gradually warming acidic and/or alkaline hydrothermal solutions (Roy, 1992). These solutions were able to leach Cu–Zn–Mn–Fe and other metals in the oceanic crust. Metal-enriched hydrothermal solutions carried towards the seafloor provided massive sulfide (Cu–Zn) deposits and manganese–ferromanganese mineralizations. The precipitation of different metals from hydrothermal solutions is associated with a decrease in pressure and temperature in the solution, and an increase in Eh and/or pH. Mixing the solution with a high amount of sea water will lower the temperature and make it more alkaline (Khan et al., 2020). The manganese oxide and sulfur mineralizations observed in the volcanic sedimentary succession of the Koçali Complex must have formed during the post-rifting oceanicization (seafloor spreading) of the southern Neotethys during the Late Triassic period (Fig. 8). The origin of the Koçali manganese mineralizations are similar to modern and ancient hydrothermal systems in mid-ocean spreading centers (Shah and Khan, 1999; Roy, 1992; Khan et al., 2020).

Compared to Mn, Fe compounds precipitate closer to the hydrothermal vents, while manganese has been reported to precipitate further away (Roy, 1992; Panagos and Varnavas, 1984; Khan et al., 2020). Considering the Fe and Mn concentrations of the mineralizations in the study area, it is probable that it consisted of a hydrothermal source. Despite the relatively high Fe content of the Kevrikevr Hill manganese,

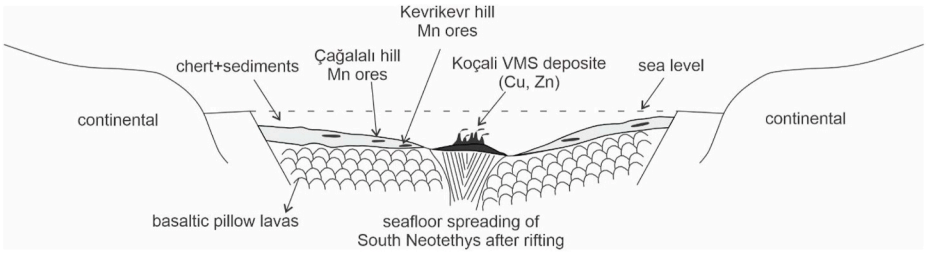


Fig. 8. Hypothetical model showing the geological formation environment of the manganese-oxide and VMS mineralizations of the Koçali Complex.

the low Mn content may indicate that they were close to the hydrothermal vents on the seafloor. Physically, the manganese mineralization of Kevrikevr Hill is located in the near west of the Koçali–VMS mineralization and is in the roof rock position. On the other hand, the very low Fe and high Mn contents of the Çağalalı Hill mineralizations were interpreted as occurring in sections more divergent from the hydrothermal vents, and a hypothetical geological environment model has been proposed (Fig. 8).

5. Conclusions

The Çağalalı Hill and Kevrikevr Hill manganese mineralizations are within the red and brown radiolarian cherts in the volcanic sedimentary series of the Koçali Complex. Pyrolusite and polianite are the main manganese minerals and contain smaller amounts of psilomelane, manganite and minor hausmannite. The gangue minerals are mainly quartz and carbonate, with minor barite. The ore–mineral association indicated hydrothermal contribution under low-temperature conditions of the submarine environment. The main, trace and REE signatures indicated that volcanism-related hydrothermal solutions that developed along the continental rift margin during and immediately after continental rifting were responsible for manganese mineralizations. All data point to the fact that the Çağalalı Hill and Kevrikevr Hill manganese mineralizations are of hydrothermal origin.

Declaration of competing interest

The authors declare that they have no known competing financial interests or personal relationships that could have appeared to influence the work reported in this paper.

Acknowledgments

This study is a part of the Master study of Burcu Gören. This study was supported by Cukurova University Scientific Research Projects Unit, with a project number 2009MMFYL63). I would like to thank the MTA General Directorate Mining Survey Department for their support.

References

Altunbey, M., Sağıroğlu, A., 1995. Characteristics and origin of koçkale-elazığ manganese mineralizations. Mineral Res. Expl. Bull. 117, 139–148.
Bamba, T., 1984. The Tokkoro Belt, a tectonic unit of the central axial zone of Hokkaido. Hokkaido Univ. Sci. J. Ser. 4, 21–75.
Bolton, B.R., Both, R., Exon, N.F., 1988. Geochemistry and mineralogy of sea floor hydrothermal and hydrogenetic Mn oxide deposits from the manus basin and bismarck archipelago region of the southwest pacific ocean. Mar. Geol. 85 (1), 65–87.
Bonatti, E., Zerbi, M., Kay, R., Rydell, H.S., 1976. Metalliferous deposits aphenine ophiolites. Geol. Soc. Am. Bull. 87, 83.
Bozkurt, E., 2001. Neotectonics of Turkey—a synthesis. Geodin. Acta 14, 3–30.
Choi, J.H., Hariya, Y., 1992. Geochemistry and depositional environment of Mn oxide deposits in the tokoro belt, Northestern Hokkaido. Japan. Econ. Geol. 87, 12.
Crerar, D.A., Namson, J., Chyi, M.S., 1982. Manganiferous the Franciscan assemblage; I, general geology, ancient and modern analogues, and implications for hydrothermal convection at oceanic spreading centers. Econ. Geol. 77 (3), 519–540.
Evensen, M.N., Hamilton, P., O'nions, R.K., 1978. Rare-earth abundances in chondritic meteorites. Geochem. Cosmochim. Acta 42, 1199.
Fitzgerald, C.E., Gillis, K.M., 2006. Hydrothermal manganese oxide deposits from baby bare seamount in the northeast pasific ocean. Mar. Geol. 225, 145.
Fourcade, E., Dercourt, J., Günay, Y., Azema, J., Kozlu, H., Bellier, J.P., Cordey, J.P., Cros, F., De Eever, P., Enay, P., Hernandez, R., Lauer, J., Vrielynck, B., 1991. Stratigraphie et paleogeographie de la margeseptentrionale de la platforme arabeau Mesozoique (Turquie de Sud-East). Bull. Soc. Geol. France 161, 27–41.
Gören, B., 2011. The Geological İnvestigates of the Manganese Depositions within the Koçali Melange (Adiyaman-Çelikhan). Msc. Thesis. Çukurova Üniv. Institute of Natural and Applied Sciences.
Gören, B., Akyıldız, M., Yıldırım, N., Ve İlhan, S., 2010. Are the manganese deposits within the Koçali melange related with Cyprus type massive sulfide deposits?. In: Abstracts of the 63rd TJK Congress, pp. p114–115. Ankara, Turkey.
Hein, J.R., Hsueh-Wen, Y., Gunn, S.H., 1994. Composition and origin of hydrothermal iron stones from central pacific seamounts. Geochem. Cosmochim. Acta 58 (1), 179–189.
Hein, J.R., Gibbs, A.E., Clague, D.A., 1996. Hydrothermal mineralization along submarine rift zones, Hawaii. Mar. Georesour. Geotechnol. 14 (2), 177–203.
Hein, J.R., Koschinsky, A., Halbach, P., 1997. Iron and manganese oxide mineralization in the pacific. In: Nicholson, K., Hein, J.R., Buhn, B., et al. (Eds.), Manganese Mineralization: Geochemistry and Mineralogy of Terrestrialand Marine Deposits. Geological Society Special Publication, pp. 123–138.
Ingram, B.L., Hein, J.R., Farmer, G.L., 1990. Age determinations and growth rates of pacific ferromanganese deposits using strontium isotopes. Geochem. Cosmochim. Acta 54 (6), 1709–1721.
İlhan, S., 2013. The Origin of Massive Sulfide Deposits within the Koçali Complex (Adıyaman). Cukurova University, p. 250p. PhD Thesis.
İlhan, S., Yıldırım, N., Akyıldız, M., Karataş, B., Dönmez, C., 2016. Isotope studies in vms deposits associated with upper triassic rifting of southern Neotethys (SE Turkey/adıyaman region). In: VII. Geochemistry Symposium. Antalya, Turkey.
Jach, R., Dudek, T., 2005. Origin of a toarcian manganese carbonate/silicate deposit from the krížna unit, tatra mountains. Poland Chem. Geology 224, 136–152.
Jiancheng, X., Yang, J., Xu, W., 2006. Geochemical characteristics of sedimentary manganese deposit of Guichi, Anhui Province, China. J. Rare Earths 24, 374.
Khan, M.A., Kakar, M.I., Ulrich, T., Ali, L., Andrew, C., Kerr, A.C., Mahmood, K., Sıddıqui, R.H., 2020. Genesis of manganese deposits in the ali khanzai block of the Zhob ophiolite, Pakistan: inferences from geochemistry and mineralogy. J. Earth Sci. 31 (5), 884–895.
Kuşcu, M., Gedikoğlu, A., 1989. Geochemical characteristics of the Ulukent (Tavas-Denizli) manganese deposits. Geologist of sound 17, 29–47.
Marta Polgári, P.M.O., 1991. Stable isotope evidence for the origin of the urkut manganese ore deposit, Hungary. SEPM J. Sedimentary Res. 61 (3), 384–393.
Mta, 2002. 1: 500 000 Scale Geology Map of Turkey. General Directorate of Mineral Research and Exploration, Ankara, Turkey.
Okay, A.I., 2008. Geology of Turkey: a synopsis. Anschnitt 21, 19–42.
Okay, A.I., Tüysüz, O., 1999. Tethyan sutures of northern Turkey. In: Durand, B., Jolivet, L., Horvath, F., Seranne, M. (Eds.), Mediterranean Basins: Tertiary Extension within the Alpine Orogen, 156. Geological Society of London Special Publication, pp. 475–515.
Öksüz, N., 2011. Geochemical characteristics of the eymir (Sorgun-Yozgat) manganese deposit, Turkey. J. Rare Earths 29 (3), 287–296.
Öksüz, N., 2018. Mineralogical findings from manganese deposits in the artova ophiolite complex, derbent-eymir area, Yozgat, Turkey, 2018 Bull. Min. Res. Exp. 156, 137–150. Ve Öztürk, H., Kasapçı, C. and Özbaş, F., 2018. Manganese Deposits of Turkey. Mineral Resources of Turkey pp 261-281.
Öygür, V., 1990. The views on Geology, deposition and genesis of manganese deposit in Çayırlı (Ankara-Haymana). Mineral Res. Expl. Bull. 110, 29–43.
Öztürk, H., Frakes, L.A., 1995. Sedimentation and diagenesis of an Oligocene manganese deposit in a shallow subbasin of the Paratethys, Thrace basin, Turkey. Ore Geol. Rev. 10, 117–132.
Öztürk, H., 1993a. Manganese mineralizations in Turkey: processes of formation and types. Geol. Eng 43, 24–33 (In Turkish with English abstract).
Öztürk, H., 1993b. Characteristics and formations of fossil manganese nodules in the Koçali Komplex, Adıyaman, Turkey. Geol. Bull. Turk. 36, 159–169 (In Turkish with English abstract).
Öztürk, H., Kasapçı, C., Özbaş, F., 2019. Manganese deposits of Turkey. In: Pirajno, F., Ünlü, T., Dönmez, C., Şahin, M. (Eds.), Mineral Resources of Turkey. Modern Approaches in Solid Earth Sciences, 16. Springer, Cham.
Panagos, A.G., Varnavas, S.P., 1984. On the genesis of some manganese deposits from eastern Greece. In: Wauschkuhn, A. (Ed.), Syngenesis and Epigenesis in the Formation of Mineral Deposits. Spriger, Berlin, pp. 553–561.

Perincek, D., 1978. The Investigation of the Geology and the Petroleum Potential of the Çelikhan-Sincik-Kocali (Adıyaman) Area. PhD Thesis. Istanbul Uni. Sci. Fac., p. 212 (in Turkish).
Peters, T., 1988. Geochemistry of manganese-bearing cherts assoicated with Alpine-ophiolites and the Hawasina formations in Oman. Mar. Geol. 84, 229.
Polgári, M., Hein, J.R., Vigh, T., 2012. Microbial processes and the origin of the Úrkút manganese deposit, Hungary. Ore Geol. Rev. 47, 87–109.
Robertson, A.H.F., Parlak, O., Yıldırım, N., Dumitrica, P., Taslı, K., 2016b. Late triassic rifting and Jurassic–cretaceous passive margin development of the southern Neotethys: evidence from the adıyaman area. SE Turkey Int. J. Earth Sci.
Robertson, A.H.F., Boulton, S.J., Taslı, K., İnan, N., Yıldırım, N., Yildiz, A., Parlak, O., 2016a. Late Cretaceous-Miocene sedimentary development of the Arabian continental margin in SE Turkey (Adıyaman Region): implications for regional palaeogeography and the closure history of Southern Neotethys. J. Asian Earth Sci.
Robertson, A.H.F., Ünlügenç, U.C., İnan, N., Taslı, K., 2004. The Misis–Andırın Complex: a Mid-Tertiary melange related tolate-stage subduction of the southern Neotethys in S Turkey. J. Asian Earth Sci. 22, 413–453.
Roy, S., 1992. Environments and processes of manganese deposition. Econ. Geol. 87 (5), 1218–1236.
Roy, S., 1997. Genetic diversity of manganese deposition in the terrestrial geological record. In: Nicholson, K., Hein, J.R., Buhn, B., et al. (Eds.), Manganese Mineralization: Geochemistry and Mineralogy of Terrestrialand Marine Deposits, 119. Geological Society of London Special Publication, pp. 5–27.
Shah, M.T., Khan, A., 1999. Geochemistry and origin of Mn-deposits in the Waziristan ophiolite complex, north Waziristan, Pakistan. Miner. Deposita 34 (7), 697–704.
Shah, M.T., Moon, C.J., 2007. Manganese and ferromanganese ores from different tectonic settings in the NW Himalayas, Pakistan. J. Asian Earth Sci. 29–455.
Şaşmaz, A., Gümüş, G., Sağıroğlu, A., 1999. A typical example of transported Cyprus type copper mineralizations: derdere (Çüngüş-Diyarbakır) mineralizations. Turkish Geology Bulletin volume 42 (issue 1), 105–117.
Şaşmaz, A., Türkyılmaz, B., Öztürk, N., Yavuz, F., Kumral, M., 2014. Geology and geochemistry of Middle Eocene Maden complex ferromanganese deposits from the Elazığ–Malatya region, eastern Turkey. Ore Geol. Rev. 56, 352–372.
Şengör, A.M.C., Yılmaz, Y., 1981. Tethyan evolution of Turkey: a platetectonic approach. Tectonophysics 75, 181–241.
Toth, J.R., 1980. Deposition of submarine crusts rich in manganese and iron. Geol. Soc. Am. Bull. 91 (1), 44–54.
Türkyılmaz, B., 2004. The Mineralogical, Geochemical and Provenance Investigation of the Manganese Deposits along the Southeast Anatolian Trust Belt. PhD thesis Fırat Univ. Instıtute of basic and applied sciences, Elaziğ, p. 160 (in Turkish).
Usui, A., Nishimura, A., 1992. Submersible observations of hydrothermal manganese deposits on the kaikata seamount, izu-Ogasawara (bonin) arc. Mar. Geol. 106 (3/4), 203–216.
Usui, A., Someya, M., 1997. Distribution and composition of marine hydrogenetic and hydrothermal manganese deposits in the northwest pacific. Geological Society, London, Special Publications 119 (1), 177–198.
Uzunçimen, S., Tekin, U.K., Bedi, Y., Perincek, D., Varol, E., Soycan, H., 2011. Discovery of the late triassic (Middle carnian–rhaetian) radiolarians in the volcano-sedimentary sequences of the Koçali complex, SE Turkey: correlation with the other taurideunits. J. Asian Earth Sci. 40 (Issue 1), 180–200, 4 January 2011.
Varentsov, I.M., 1993. Distribution of rare earth elements in Mn-Fe Oxyhydroxide crusts from bezymiannaya seamount, atlantic: geochemical history of deposition. Chem. Erde 53, 133–157.
Von, S., 1997. Growth History of Manganese Nodules and Crusts of the Peru Basin Geological Society. Special Publications, London, pp. 119–153.
Yazgan, E., Cheessex, R., 1991. Geology and tectonic evolution of the southestern Taurides in the region of malatya. Tür. Pet. Jeo. Der., Ankara 3 (1), 1–14.
Yıldırım, N., İlhan, S., Yıldırım, E., Dönmez, C., 2012. The geology, geochemıstry and genetical features of the Ormanbaşı Hill (sincik, adıyaman) copper mineralization. Mineral Res. Expl. Bull. 144, 75–104.
Yıldırım, N., 2013a. Mining Potential of Adıyaman Province. Mining Symposium of Malatya and Surrounding Provinces. Book of proceedings. Page 1.
Yıldırım, N., 2013b. "SE Anatolian Cyprus Type VMS Metallogenic Belt" Discovered in the Scope of Basin-Belt Mining: Koçali Complex, Adıyaman Region, SE Turkey. MTA Natural Resources and Economy Bulletin, Ankara issue:14.
Yıldırım, N., 2017. Petrological Characteristics and Tectonic Importance of Oceanic Units Forming the Koçali Complex (Adıyaman). Cukurova University. PhD Thesis.
Yıldırım, N., Dönmez, C., Kang, J., Lee, I., Pirajno, F., Yıldırım, E., Günay, K., Seo, J.H., Farquhar, J., Chang, S.W., 2016. A magnetite-rich Cyprus-type VMS deposit in Ortaklar: a unique VMS style in the Tethyan metallogenic belt, Gaziantep, Turkey. Ore Geol. Rev. 79, 425–442. December 2016.
Yılmaz, Y., 1990. Allochtonous Terranes in the Tethyan Middle East: Anatolia and Surrounding Regions, A331. Royal Soc. London Phyl Trans, pp. 611–624.
Yılmaz, Y., 1993. New evidence and model on the evolution of the southeast Anatolian orogen. Geol. Soc. Am. Bull. 105, 251–271.
Yılmaz, Y., Yiğitbaş, E., Genç, Ş.C., 1993. Ophiolitic and metamorphic assemblages of Southeast Anatolia and their significance in the geological evolution of the orogenic belt. Tectonics 12, 1280–1297.